Anomalous Behavior of Unplasticized PVC Compounds in Capillary Flow

NOBUYUKI NAKAJIMA and EDWARD A. COLLINS, *B. F. Goodrich Chemical Company, Technical Center, Avon Lake, Ohio 44012*

Synopsis

Capillary rheometry was performed over a temperature range of 170°–200°C and a shear-rate range of 3–3000 sec^{-1} on an unplasticized poly(vinyl chloride) compound. The data were corrected for the effect of pressure on viscosity, for pressure loss in the barrel and at the capillary entrance, and for the non-Newtonian velocity profile. The pressure coefficient of viscosity was found to be in the same order of magnitude as those previously found with linear polyethylene and butadiene-acrylonitrile copolymers. The pressure–shear-rate superposition of the flow curves is valid at least approximately, although the temperature–shear-rate superposition is inapplicable. The shape of flow curves at 180°, 190°, and 200°C are concave downward when they are expressed as log-shear-stress–log-shear-rate. Similar plots at 170° and 175°C, however, are very different; shear stress is independent of shear rate at low shear rates, increases somewhat and becomes independent of shear rate again at high shear rates. There is no detectable temperature dependence of flow behavior at 170° and 175°C. Irregularly shaped extrudates were obtained at higher shear rates. At constant shear rate the irregularity increased with the length of the capillary. The effect of thermal-mechanical history on the particulate and crystalline structure is discussed with possible influence on the reproducibility of the rheological data.

INTRODUCTION

Unplasticized poly(vinyl chloride) (PVC) is used in large quantity for fabricating rigid objects, such as pipes, bottles, and building materials. Processing of the compound involves extrusion or injection molding over a very wide temperature range up to, and in some cases above, the melting point. Several papers have been published on the capillary rheometry of PVC compounds.[1–6] This study focuses attention on the rheology of PVC compound in the temperature range below the melting point, i.e., between 170° and 200°C. The study was designed to explore the effect of capillary viscometer extrusion variables, primarily shear rate, temperature, and various capillary L/D ratios. In the temperature range considered, it is known that the material possesses a particulate and crystalline structure,[7–11] which may be altered by heat and mechanical action. The presence of particulate and crystalline structure differentiates the flow of this material from that of amorphous melts of thermoplastics such as poly(ethylene) and poly(styrene). Two differences in the flow behavior were observed by capillary rheometry. First, the PVC compound has a much higher temperature dependence of the viscosity compared to amorphous molten polymers; and second, the shape of the flow curve depends on the temperature and, therefore, the temperature reduction scheme[12] is not applicable to these flow curves.

This study is directed to investigate additional differences in the flow behavior including the effect of pressure on the viscosity, the increase in diameter of the extrudates and the distortion of the extrudates.

Journal of Applied Polymer Science, Vol. 22, 2435–2449 (1978)

0021-8995/78/0022-2435$01.00

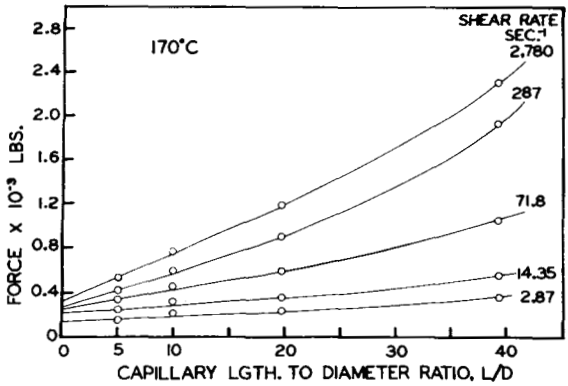

Fig. 1. Pressure vs capillary L/D at constant shear rate at 170°C.

EXPERIMENTAL

Sample

The PVC compound was a commercial product for injection molding. The resin in the compound has an inherent viscosity of 0.67 in cyclohexanone at 0.2 g/dl concentration and 30°C. The granules were prepared by milling at 170°C.

A commercial extrusion compound was also examined to find the effect of thermal-mechanical history on flow. The resin in this compound has an inherent viscosity of 1.13 measured at the same condition as above.

Instrument and Operation

An Instron capillary rheometer was used with four dies having diameters of 0.050 in. and L/D ratios of 5.08, 10.1, 19.8, and 39.4. The measurements were made at 170°, 175°, 180°, 190°, and 200°C.

The shear rate range was 2.9–2900 sec^{-1}. With a single charge of material, the machine was operated to give ten different speeds, according to a preset program. It was run from low to high speed. The program was set so that the melt height in the barrel was the same at a given drive speed. This provides an

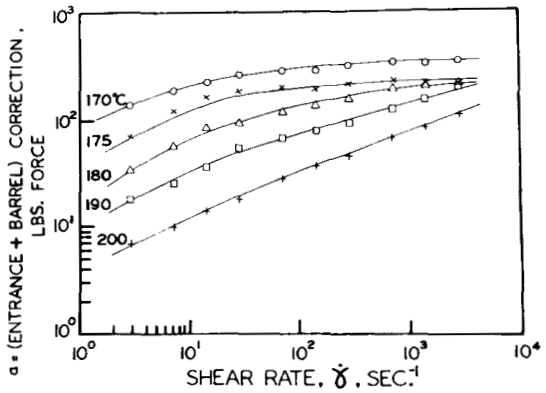

Fig. 2. Pressure loss (expressed as force) at entrance and barrel as a function of shear rate.

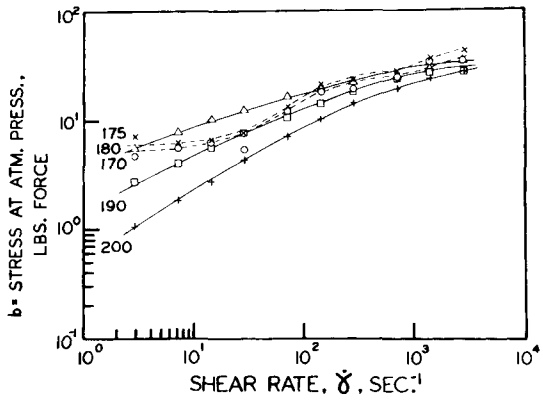

Fig. 3. Shear stress (expressed as force) at atmospheric pressure as a function of shear rate.

advantage in making the barrel and entrance corrections together in one step, as will be shown later.

RESULTS

Flow Data

The observed results at 170°C are presented in Figure 1, where the force F lbs on the plunger is plotted against L/D of the capillary at each shear rate (drive speed). The pressure on the plunger is the force divided by the surface area of the plunger (0.1104 in.^{2} for the instrument used).

The force extrapolated to zero L/D corresponds to the combination of barrel and entrance pressure loss, because the amount of material remaining in the barrel is the same regardless of the L/D of the capillary. This treatment assumes the affects of hydrostatic pressure on these losses are negligible.

Practically all the curves at all temperatures showed the upward swing at large L/D values. This viscosity increase is interpreted to be caused by hydrostatic pressure.[13]

The data were fitted using the following three-parameter equation:

$$F = a + b(L/D) + c(L/D)^2 \tag{1}$$

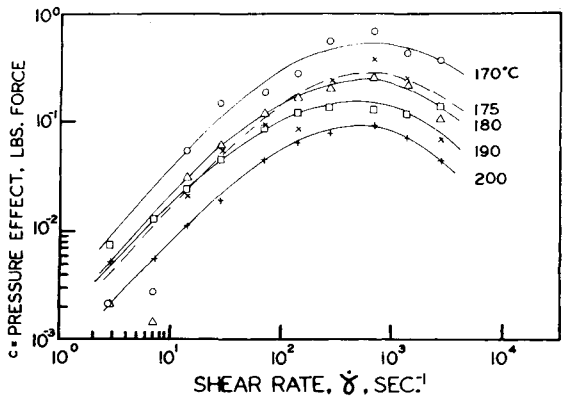

Fig. 4. Effect of pressure (expressed as force) on flow at constant shear rate.

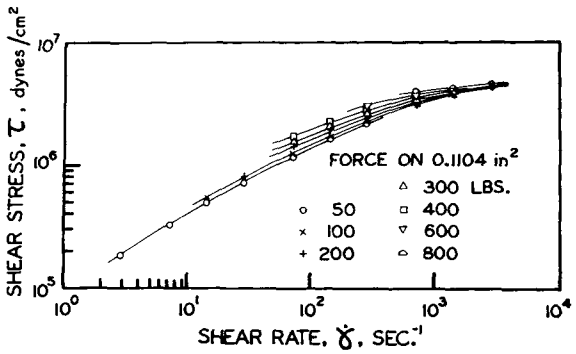

Fig. 5. Shear stress vs shear rate at different pressures at 200°C.

where a corresponds to the barrel and entrance pressure loss, b represents the shear stress at atmospheric pressure, and c is the effect of hydrostatic pressure. Here a, b, and c are expressed in lbs force unit; but they may be converted to other appropriate units. The values of a, b, and c were obtained by the best fit to the observed data of F vs L/D. Then, the reverse calculations were made with these constants and L/D. The calculated values of F were in good agreement with the observed values and well within the experimental error. The three constants are shown as functions of shear rate in Figures 2–4. The entrance and barrel pressure losses (Fig. 2) increased with shear rate. This trend is most marked at 200°C. At the lower temperatures, the trend becomes less, particularly at higher shear rates.

Figure 3 is analogous to the usual shear-stress–shear-rate curves. The curves at 180°, 190°, and 200°C have familiar shapes typical of PVC behavior. The curves at 170° and 175°C are very different in shape from the curves at the higher temperatures, and similar to the curves of carbon black-filled elastomers.[14] This is probably an indication of the gross particulate nature of the flow units.

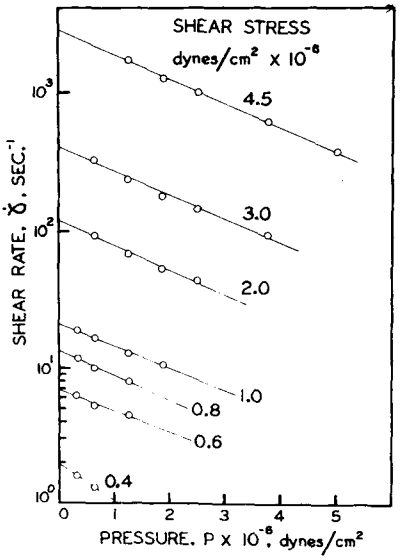

Fig. 6. Effect of pressure on flow at 190°C and constant shear stress.

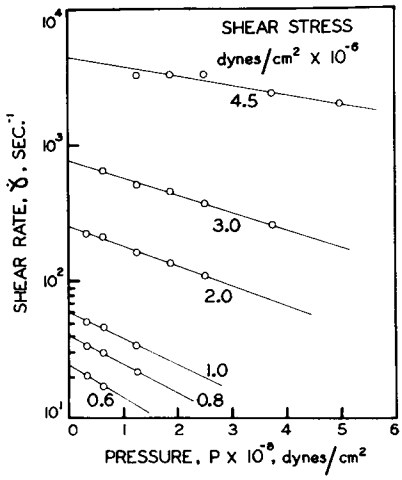

Fig. 7. Effect of pressure on flow at 200°C and constant shear stress.

The data points in Figure 4 are somewhat more scattered, because the values of c were evaluated from relatively small changes in slope. Values at low shear rates are very small and the scattering is excessive. Therefore, smoothed curves are drawn through the points. The curves at 170° and 175°C are parallel; those at 190° and 200°C are also parallel to each other but the two sets have different shapes. The curve at 180°C is almost the same as that at 175°C.

Effect of Hydrostatic Pressure on Flow

Once b and c are known for a given shear rate $\dot{\gamma}$ and temperature, the shear stresses τ dyn/cm^2 at different hydrostatic pressures may be estimated. This is done according to the following equation:

$$\tau = \frac{6.89 \times 10^4}{0.1104 \times 4}[b + 2C(L/D)] \tag{2}$$

using the L/D value corresponding to a given hydrostatic pressure in Figure 1. In this procedure, the bulk relaxation is assumed to be slower than the flow time through the capillary, so that the effect of pressure on viscosity is unchanged during the flow. This may tend to underestimate the pressure effect. The calculations were done at seven pressure levels between 30.8 and 493 atm. Then, the shear-stress–shear-rate curve was plotted at each pressure level. An example is shown in Figure 5. Interpolation of the curves at different pressure levels at constant shear stress yields a plot of $\log_{10}\dot{\gamma}$ vs pressure. Such a plot was found to be linear for polyethylene[13] and butadiene-acrylonitrile elastomers.[15] Present examples of the plots are shown in Figures 6 and 7 for the data at 190 and 200°C, respectively. The plots are found to be linear at these temperatures as well as the other temperatures examined, namely, 170°, 175°, and 180°C.

From the slopes of these plots the pressure-dependent shift factors α_p may be obtained. For constant temperature and stress conditions, the following relationship holds:

$$\frac{d \log_{10}\alpha_p}{dp} = \frac{d \log_{10}\dot{\gamma}}{dp} = -\frac{d \log_{10}\eta}{dp} \tag{3}$$

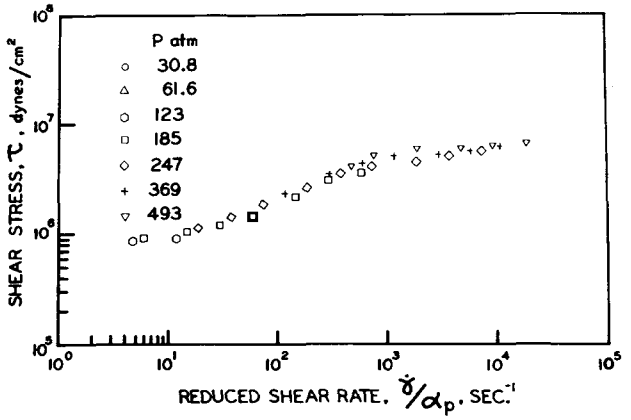

Fig. 8. Pressure superposition of flow curves at 170°C.

With polyethylene[13] and butadiene-acrylonitrile elastomers,[15] $d \log_{10}\alpha_p/dp$ values were independent of the stress levels. The data in Figure 6 suggest the same but those in Figure 7 do not. However, the slope at the lower stresses are not as accurate because only a few data points are available.

In the foregoing calculations, it was assumed that $d \log_{10}\alpha_p/dp$ was independent of temperature and stress levels. An average value 1.63×10^{-9} $(\text{dyn/cm}^2)^{-1}$, of $d \log_{10}\alpha p/dp$ was used. If the above assumption is correct, the flow data at different pressures must superpose each other when the shear rates are reduced to those at a reference pressure by applying the shift factor α_p.

The results of such calculations are shown in Figures 8 and 9, where the reference pressure is taken as atmospheric pressure. The value of α_p at each pressure p was calculated by

$$\log_{10}\alpha_p = \frac{d \log_{10}\alpha_p}{dp} \times p \tag{4}$$

and the shear rates $\dot{\gamma}$ at each pressure were reduced by $\dot{\gamma}/\alpha_p$. The superpositions of data in a form of $\tau \sim \dot{\gamma}/\alpha_p$ plots are good at 180°, 190°, and 200°C. They may also be valid at 170° and 175°C, because the scattering of the points may be within experimental error.

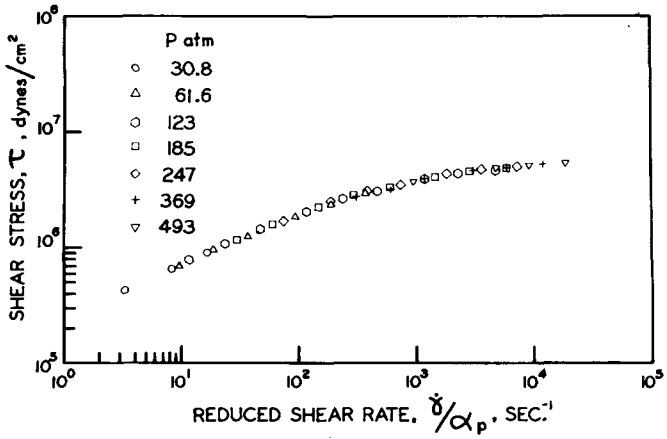

Fig. 9. Pressure superposition of flow curves at 190°C.

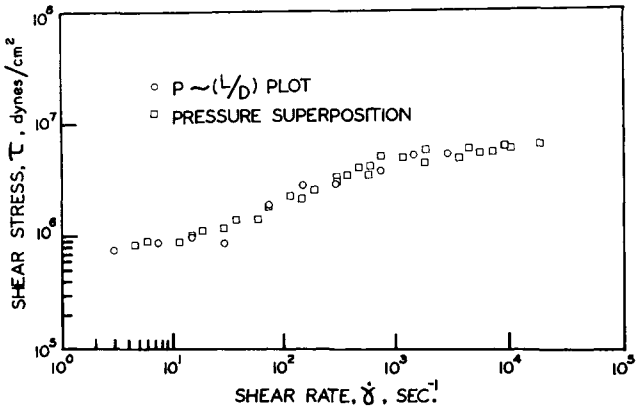

Fig. 10. Shear stress at atmospheric pressure at 170°C calculated by two different methods.

The curves of Figures 8 and 9 may be calculated quite differently without going through the number of steps described above; namely, the plot of $b \sim \dot{\gamma}$ (Fig. 3) may be converted to a $\tau \sim \dot{\gamma}$ plot as follows:

$$\tau \text{ (dyn/cm}^2\text{)} = b \text{ (lbs)} \frac{6.89 \times 10^4}{0.1104 \text{ (in.}^2\text{)}} \times \frac{1}{4} \tag{5}$$

The results of this calculation are compared with the data from the pressure superpositions in Figures 10 and 11. The agreement between two sets of data is quite good. Therefore, the assumptions made in the pressure superpositions are at least approximately correct.

The data at 170° and 175°C are shown together in Figure 12. The curves at 180°, 190°, and 200°C, given in Figure 13, show the usual temperature dependence for PVC. However, at 170° and 175°C not only is the shape of curve different from those at the higher temperature but they also have no temperature dependence.

A further correction was made to the shear rates to correct for the non-Newtonian nature of the flow and these are expressed as the shear rates at the capillary wall.[16] Because the shear-stress values were those at the capillary wall, the corrected flow data are a more precise representation of the flow behavior. The corrected curves are shown in Figure 14 as the viscosity–shear-rate curves.

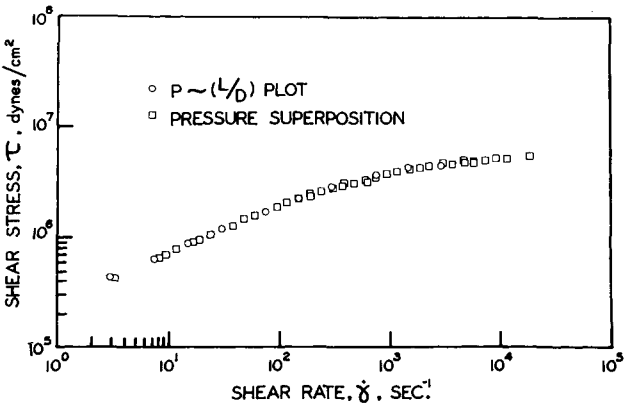

Fig. 11. Shear stress at atmospheric pressure at 190°C calculated by two different methods.

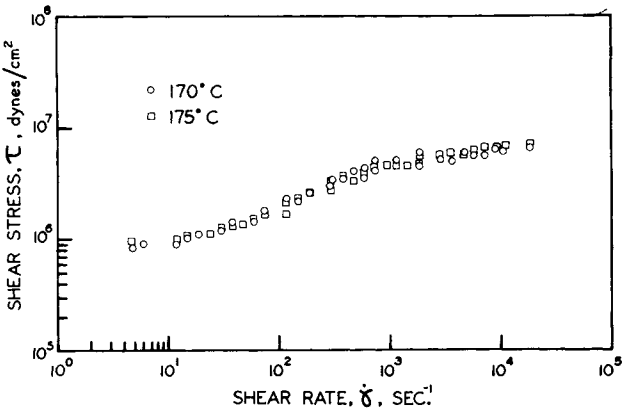

Fig. 12. Shear stress vs shear rate at 170° and 175°C and atmospheric pressure.

For the shear-rate range of extrudate distortion, this treatment should be understood to be only approximation.

Diameter and Appearance of Extrudates

An increase in diameter of the extrudate upon extrusion from a capillary is commonly observed with thermoplastic melts. The magnitude of the increase may be a factor of 2 or more.[17] With the present examples, it is rather small, 1.1–1.4; the magnitude is very similar to that observed with the carbon black-filled elastomers.[14] The observed values are plotted in Figure 15 as a function of shear rate. The data with capillaries of L/D = 5 and 40 are shown. Those with L/D = 10 and 20 fall between the two curves. In general, the value decreases with increase in L/D and increases with increasing shear rate. These trends are the same as those observed with thermoplastic melts.[17] However, for L/D = 40° at 190°C, the post-extrusion swell is independent of shear rate, and at 200°C, it decreases with shear rate. Apparently at the higher temperature the memory relaxes more rapidly, particularly at the higher shear rates. Since PVC has a broad melting range, this behavior at 200°C may be related to partial melting.

The smallest value of the diameter increase is 1.1; it is similar to the value

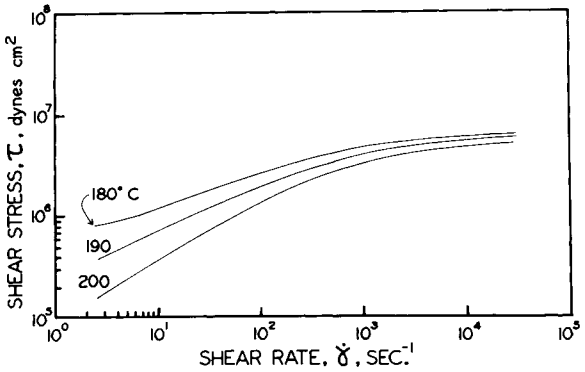

Fig. 13. Shear stress vs shear rate at 180°, 190°, and 200°C and atmospheric pressure.

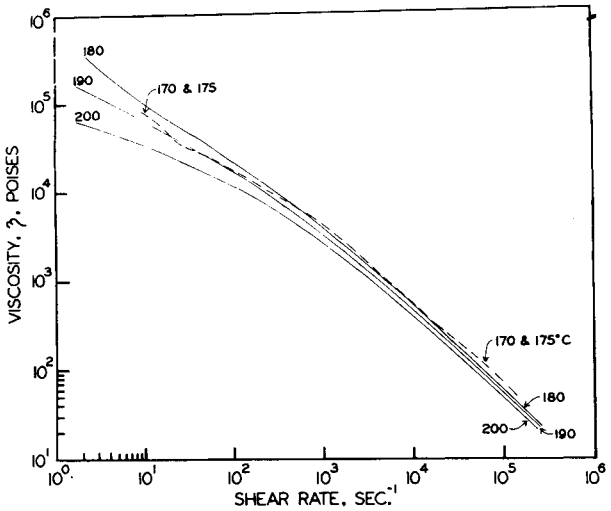

Fig. 14. Viscosity vs shear rate corrected for non-Newtonian velocity profile at atmospheric pressure.

predicted for Newtonian inelastic fluids.[18] However, the present material exhibits behavior far from Newtonian flow (Fig. 14), even at the lowest shear rate of observation.

The appearance of the extrudates varied from a uniform cylinder to irregular ones; the manner and extent of irregularity are illustrated in the photograph shown in Figure 16. The surface gloss also changes, depending upon the extrusion conditions.

The results are summarized in Table I, where S is designated for a smooth surface and R for a rough surface as measured by passing ones fingers over the surface. Wherever the symbol D is used, the extrudates were not uniform cylinders but irregularly shaped as shown in Figure 16.

In general, the extrudate distortion and the surface roughness were observed at the higher shear rates. Also, they were more extensive at the lower temperature. These trends are the same as those with other polymer melts. The sur-

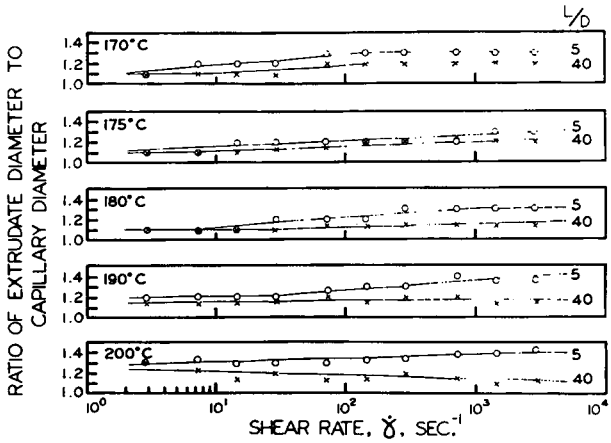

Fig. 15. Extrudate diameter as a function of shear rate.

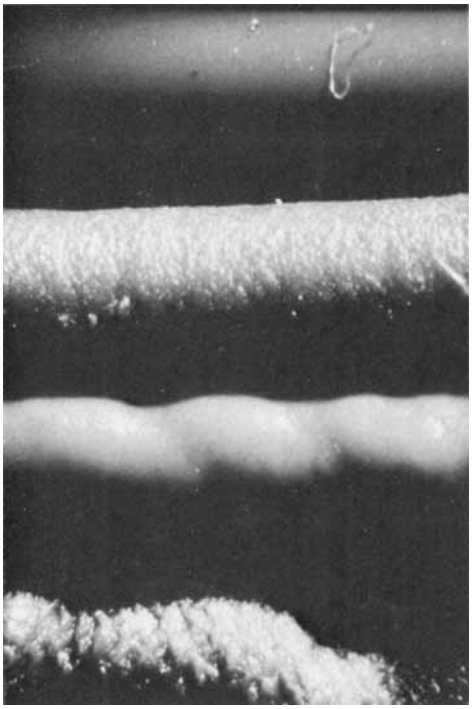

Fig. 16. Appearance of extrudates.

face roughness, as well as the distortions, were intensified with the longer capillaries. This fact is again similar to the behavior of carbon black-filled elastomers.[14] It indicates that the roughness and distortions did not occur at the entrance to the capillary, as is interpreted in some cases with molten polymers.[19] If it occurs at the entrance, the longer capillary would have smoothed the distortion or at least they would not have been intensified. The difference in appearance of the extrudates at 170° and 175°C implies that the elasticity at these temperatures may be different, although viscosities are the same. The magnitude of the entrance corrections (Fig. 2) also implies the difference in elasticity.

DISCUSSION

Temperature Dependence of Viscosity

Figure 17 is a plot of the viscosity at a fixed shear stress as a function of reciprocal absolute temperature. The data were taken from Figure 14. With most polymer melts, these type of plots give straight lines with a slope independent of the shear stress. With the present example, two peculiarities are noted: first, there appears to be a certain transition between 175° and 180°C. Below this the viscosities are independent of temperature, at the transition the viscosities tend to increase and above this transition the viscosity decreases. The second point is that the temperature dependence of the viscosity above the transition further depends on the shear stress. This behavior is most probably a manifestation of structure changes, particulate, and crystalline, which are sensitive

TABLE I
Appearance of Extrudates

Temperature (°C)	L/D	Shear rate (sec^{-1}) 2.9	7.2	14.4	28.7	71.8	144	287	718	1440	2900
170	5.08	S	S	S	S	S	S	D,S	D,S	D,S	D,R
	10.1	S	S	S	S	S	D,S	D,S	D,S	D,R	D,R
	19.8	S	S	S	S	D,S	D,S	D,S	D,S	D,R	D,R
	39.4	S	S	S	D,S	D,S	D,S	D,S	D,S	D,R	D,R
175	5.08	S	S	S	S	S	S	S	S	D,R	D,R
	10.1	S	S	S	S	S	S	S	D,R	D,R	D,R
	19.8	S	S	S	S	S	S	S	D,S	D,R	D,R
	39.4	S	S	S	S	S	D,S	D,S	D,S	D,R	D,R
180	5.08	S	S	S	S	S	S	S	S	S	R
	10.1	S	S	S	S	S	S	S	S	R	R
	19.8	S	S	S	S	S	S	S	D,S	D,R	D,R
	39.4	S	S	S	S	S	S	S	D,S	D,R	D,R
190	5.08	S	S	S	S	S	S	S	S	S	R
	10.1	S	S	S	S	S	S	S	S	S	R
	19.8	S	S	S	S	S	S	S	S	S	R
	39.4	S	S	S	S	S	S	S	S	D,R	D,R
200	5.08	S	S	S	S	S	S	S	S	S	S
	10.1	S	S	S	S	S	S	S	S	S	S
	19.8	S	S	S	S	S	S	S	S	S	R
	39.4	S	S	S	S	S	S	S	S	R	R

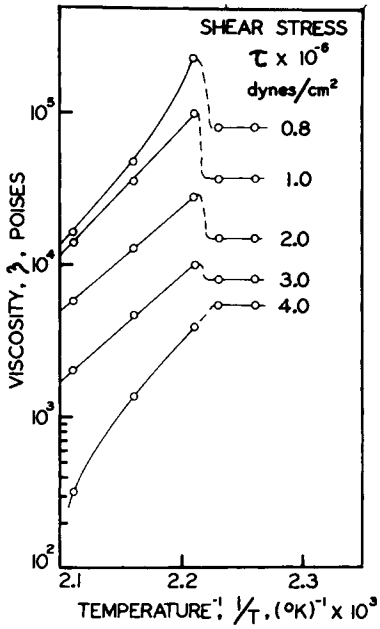

Fig. 17. Effect of temperature on viscosity at atmospheric pressure and constant shear stress.

to heat and mechanical history. Below the transition, the structure is relatively stable within the time of observation. The increase of viscosity at the transition may be caused by the melting of crystallites and subsequent recrystallization to more stable crystallites.[20] The transition temperature 175°–180°C is probably dependent on the previous thermal-mechanical history, i.e., the granulation at approximately 170°C.

Reproducibility of the Rheological Behavior

The above interpretation indicates that the flow behavior of PVC between 180° and 200°C is affected by thermal and mechanical history of the sample. If so, the same PVC sample, but having a different thermal and mechanical history, must exhibit different flow behavior under identical extrusion conditions. Further, if the melting and recrystallization to a more stable structure is occurring, giving an increase in viscosity, then a sample having received a longer heat history at this temperature range should give a higher viscosity. In order to investigate this aspect, first, reproducibility of the flow behavior was examined with essentially the same thermal-mechanical history on the sample. Then, a different history was given to the sample and the difference in flow behavior was observed.

Temperatures of 175° and 180°C and capillaries with L/D ratios of 39.4 and 19.8 were selected for this study because the material behavior appeared to be most variable at these conditions. The reproducibility of the force response in duplicate runs at each shear rate is shown in Figure 18(a) and 18(b). With these and foregoing examples, no corrections are applied to the flow data. For an L/D of 19.8, the errors were rather large, whereas the data were reproduced very well at an L/D of 39.4. The duplicate runs may not necessarily yield sufficient information on reproducibility. A larger number of runs must be made. In Figure

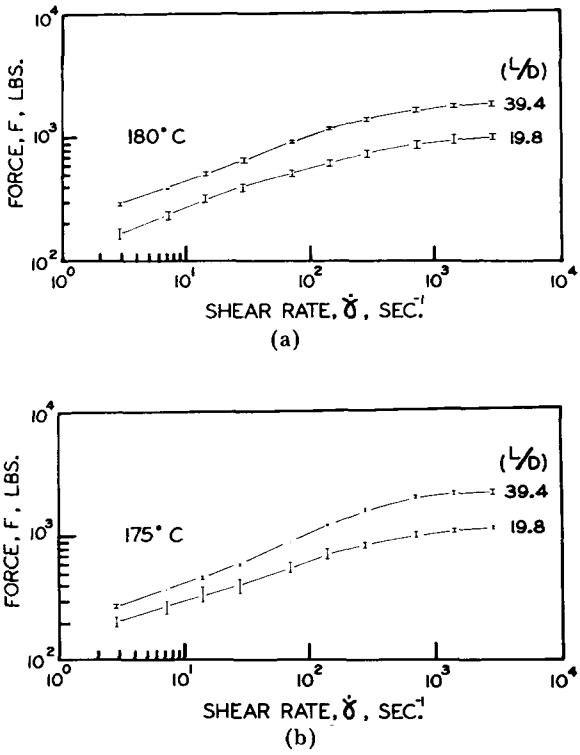

Fig. 18. Reproducibility of flow data at 175° and 180°C for an L/D of 19.8 and 39.4.

19, the reproducibility of six runs is shown with a different compound (standard commercial pipe compound) at 180°C using an L/D of 39.4. Figure 19(a) shows the extremes of six runs and Figure 19(b) shows the results of two runs which agreed very well with each other. With these particular runs, the errors were larger at the lower shear rates. The good agreement of results of two runs [Fig. 19(b)] is obviously fortuitous. The extent of error is rather large compared to, for example, the capillary extrusion of polyethylene. With PVC, even with a standarized operating procedure, the sample may have a somewhat different heat history because of the variation in the manner by which sample is charged and preheated before the flow data are taken.

Figure 20 shows the results of runs with a die having an L/D of 10. The entrance corrections are the same because its L/D is the same. The barrel corrections are essentially the same because the barrel height, at a given shear rate, is arranged to be essentially the same. Therefore, the reproducibility may be analyzed without making the above corrections. All these runs were made from the lower shear rate to the higher shear rates, as were all other experiments in this work. The lower the starting shear rate, the higher was the viscosity at a given shear rate. This may be interpreted that the longer the time of exposure at 190°C, the higher the viscosity. The largest disagreements were found in the shear rate range of 10^0–10^2 sec^{-1}. These observations are in agreement with the interpretation that the flow behavior of PVC in the 180°–200°C range is affected by the thermomechanical history of the sample.

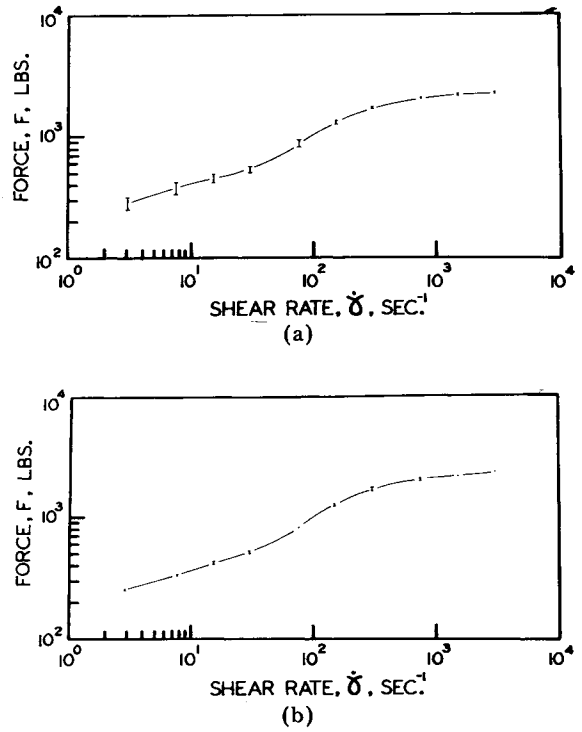

Fig. 19. Reproducibility of flow data at 180°C for an L/D of 39.4; extreme values and best agreements.

Pressure Dependence of Viscosity

For amorphous polymers, it was observed that the temperature dependence and pressure dependence have the same form. This is not surprising, since both functions are related to density change. With the structured material of this work, we do not know at present if the structures are sensitive to pressure-time as well as temperature-time history. The applicability of pressure-superposition has been demonstrated in a previous section. This would suggest that the structures in the PVC compound are not appreciably affected by the static pressure. However, this statement is not exactly correct, since it is known that the melting temperature and annealing of crystallites are affected by static pressure.

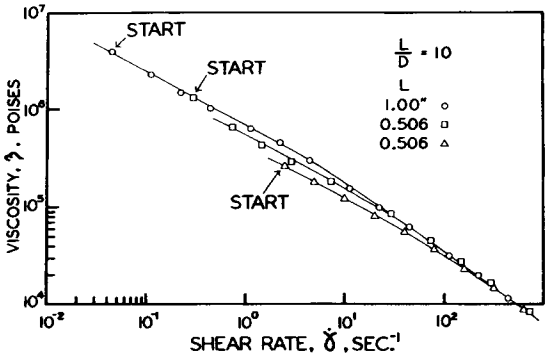

Fig. 20. Effect of thermomechanical history on flow data at 190°C.

Assuming that no appreciable structure change occurs due to the hydrostatic pressure, the pressure dependence of viscosity at constant shear stress may be expressed as

$$\frac{d \log_{10}\eta}{dp} = \frac{d \log_{10}\alpha_p}{dp} = \frac{d \log_{10}\dot{\gamma}}{dp} = \frac{B}{2.303} \tag{6}$$

The average value of B is 3.75×10^{-9} $(\text{dyn/cm}^2)^{-1}$ or 2.6×10^{-4} $(\text{psi})^{-1}$. The value is the same order of magnitude as that observed for a linear polyethylene[13] 1.6×10^{-4} $(\text{psi})^{-1}$ and those for butadiene-acrylonitrile copolymers[15] (1.7–2.2) $\times 10^{-4}$ $(\text{psi})^{-1}$. These values may be related to the stiffness of the polymer chains. The interpretation being analogous to the magnitude of flow activation energies of amorphous polymers; i.e., the higher the values of the activation energy or the pressure coefficient, the stiffer is the polymer chains.

Additional measurements are needed to verify the hypothesis in this work. In particular, supporting studies by electron microscopy on fractured specimens and perhaps small-angle x-ray diffraction should shed further insight into the anomalous behavior observed.

The authors are indebted to R. G. Raike for the capillary rheometry data, to R. Lasch for the computer calculations, to J. B. Haehn for the inherent viscosities and to A. P. Metzger for helpful discussions. The authors are grateful to B. F. Goodrich Chemical Company for permission to publish this work.

References

1. C. L. Sieglaff, *Polym. Eng. Sci.*, **9**, 81 (1969).
2. E. A. Collins and A. P. Metzger, *Polym. Eng. Sci.*, **11**, 446 (1971).
3. L. A. Utracki, Z. Bakerdjian, and M. R. Kamal, *Trans, Soc. Rheol.*, **19**, 173 (1975).
4. J. L. S. Wales, *J. Polym. Sci., Symp.* No. 50, 469 (1975).
5. P. L. Shah, *SPE Trans.*, **27**, 49 (1971).
6. P. L. Shah, *Polym. Eng. Sci.*, **14**, 773 (1974).
7. A. R. Berens and V. L. Folt, *Trans. Soc. Rheol.*, **11**, 95 (1967).
8. A. R. Berens and V. L. Folt, *Polym. Eng. Sci.*, **8**, 5 (1968).
9. A. R. Berens and V. L. Folt, *Polym. Eng. Sci.*, **9**, 27 (1969).
10. E. A. Collins and C. A. Krier, *Trans. Soc. Rheol.*, **11**, 225 (1967).
11. E. A. Collins and A. P. Metzger, *Polym. Eng. Sci.*, **10**, 57 (1970).
12. J. D. Ferry, *Viscoelastic Properties of Polymers*, 2nd ed., Wiley, New York, 1970, p. 300.
13. S. Y. Choi and N. Nakajima, *Proceedings of the Fifth International Congress on Rheology*, Vol. 4, S. Onogi, Ed., University Park Press, University Park, Pa., 1970, p. 287.
14. N. Nakajima and E. A. Collins, *Rubber Chem. Technol.*, **48**, 615 (1975).
15. N. Nakajima and E. A. Collins, *Polym. Eng. Sci.*, **14**, 137 (1974).
16. B. Rabinowitsch, *Z. Phys. Chem. A*, **145**, 1 (1929).
17. N. Nakajima and M. Shida, *Mechanical Behavior of Materials, Proceedings of the 1971 International Conference on Mechanical Behavior of Materials*, Publisher, City, 1972, Vol. III, p. 485.
18. W. W. Graessley, S. D. Glasscock, and R. L. Crawley, *Trans. Soc. Rheol.*, **14**(4), 519 (1970).
19. E. B. Bagley and H. P. Schreiber, *Elasticity Effect in Polymer Extrusion in Rheology*, Vol. 5, F. R. Eirich, Ed., Academic, New York, 1969, pp. 93–125.
20. K. H. Illers, *Makromol. Chem.*, **127**, 1 (1969); and F. Rybniker, *ibid.*, **140**, 91 (1970).

Received October 27, 1976
Revised March 29, 1977